Converting GLX2-1 into an active glyoxalase II

ARTICLE *in* BIOCHEMISTRY · SEPTEMBER 2010

Impact Factor: 3.02 · DOI: 10.1021/bi1010865 · Source: PubMed

8 AUTHORS, INCLUDING:

Melissa G Naylor
University of Chicago
11 PUBLICATIONS **142** CITATIONS
SEE PROFILE

Brian Bennett
Marquette University
124 PUBLICATIONS **2,818** CITATIONS
SEE PROFILE

Christopher A Makaroff
Miami University
95 PUBLICATIONS **2,892** CITATIONS
SEE PROFILE

Michael W Crowder
Miami University
106 PUBLICATIONS **2,619** CITATIONS
SEE PROFILE

Published in final edited form as:
Biochemistry. 2010 September 21; 49(37): 8228–8236. doi:10.1021/bi1010865.

Converting GLX2-1 into an active glyoxalase II[†]

Pattraranee Limphong[‡], **Nicole E. Adams**[‡], **Matthew F. Rouhier**[‡], **Ross M. McKinney**[‡], **Melissa Naylor**[‡], **Brian Bennett**[§], **Christopher A. Makaroff**[‡], and **Michael W. Crowder**[‡,*]

[‡]160 Hughes Hall, Department of Chemistry and Biochemistry, Miami University, Oxford OH 45056

[§]National Biomedical EPR center, Department of Biophysics, Medical College of Wisconsin, Milwaukee, Wisconsin 53226

Abstract

Arabidopsis thaliana glyoxalase 2-1 (GLX2-1) exhibits extensive sequence similarity with GLX2 enzymes but is catalytically inactive with SLG, the GLX2 substrate. In an effort to identify residues essential for GLX2 activity, amino acid residues were altered at positions 219, 246, 248, 325, and 328 in GLX2-1 to be the same as those in catalytically-active human GLX2. The resulting enzymes were over-expressed, purified, and characterized using metal analyses, fluorescence spectroscopy, and steady-state kinetics to evaluate how these residues affect metal binding, structure, and catalysis. The R246H/N248Y double mutant exhibited low level S-lactoylglutathione hydrolase activity, while the R246H/N248Y/Q325R/R328K mutant exhibited a 1.5- to 2-fold increase in k_{cat} and a decrease in K_m as compared to the values exhibited by the double mutant. In contrast the R246H mutant of GLX2-1 did not exhibit glyoxalase 2 activity. Zn(II)-loaded R246H GLX2-1 enzyme bound 2 equivalents of Zn(II), and ^{1}H NMR spectra of the Co(II)-substituted analog of this enzyme strongly suggests that the introduced histidine binds to Co(II). EPR studies indicate the presence of significant amounts a dinuclear metal ion-containing center. Therefore, an active GLX2 enzyme requires both the presence of a properly-positioned metal center and significant non-metal, enzyme-substrate contacts, with tyrosine 255 being particularly important.

The glyoxalase system consists of two enzymes, lactoylglutathione lyase (GLX1) and hydroxyacylglutathione hydrolase (GLX2). GLX1 is capable of forming S-(2-hydroxyacyl) glutathione (SLG), which is produced from a thiohemiacetal that is formed from the spontaneous reaction of methylglyoxal with glutathione. SLG is then hydrolyzed by GLX2 to produce lactate and glutathione. GLX1 can utilize a number of α-ketoaldehydes; however, methylglyoxal (MG), a cytotoxic and mutagenic compound formed primarily as a byproduct of carbohydrate and lipid metabolism and from triose phosphates, is thought to be the primary physiological substrate of the system(1-5). SLG can also be metabolized by γ-glutamyltransferase and dipeptidase, which generate N-*D*-lactoylcysteine that passes from cell to cell and can inhibit nucleotide synthesis(6) and ultimately DNA synthesis (7). Therefore, the glyoxalase system, which depletes MG and SLG, is critical for cellular detoxification in aerobic organisms (6).

[†]This work was supported by the National Institutes of Health (AI056231 to BB, and EB001980 to the Medical College of Wisconsin), Miami University/Volwiler Professorship (to MWC), Presidential Academic Enrichment fellowship (to PL), and the National Institutes of Health GM076199 (to CAM).

[*]To whom correspondence should be addressed: Michael W. Crowder crowdemw@muohio.edu phone: (513) 529-7274 fax: (513) 529-5715.

GLX1 from a number of sources has been studied extensively using biochemical, computational, and X-ray crystallographic approaches (8). In contrast, GLX2 has been considerably less well-characterized. In humans, a single gene encodes the mitochondrial and cytoplasmic forms of GLX2 (9). On the other hand, *Arabidopsis thaliana* contains four putative GLX2 genes, including multiple mitochondrially-localized forms of GLX2 (GLX2-1, GLX2-4, and GLX2-5), as well as a gene for a cytosolic enzyme (GLX2-2) (10). The presence of multiple putative mitochondrial GLX2 enzymes is surprising because GLX1 and SLG have only been observed in the cytosol of cells (11,12). Subsequent studies confirmed that GLX2-2 and GLX2-5 are in fact GLX2 isozymes and that they contain dinuclear metal binding sites (1,13,14).

The crystal structures of human cytoplasmic and plant mitochondrial GLX2 (GLX2-5) (Figure 1) showed that the metal binding and active sites of GLX2 are most similar to that of metallo-β-lactamase L1 from *Stenotrophomonas maltophilia* (1,15,16). One of the metal binding sites (Zn_1 site) consists of three conserved histidine residues, a bridging aspartic acid, and a bridging water/hydroxide. The second metal-binding site (Zn_2 site) has 2 histidines, 1 bridging Asp, a non-bridging Asp, a terminally-bound water, and the bridging hydroxide/water. It was initially hypothesized that human GLX2 contains a dinuclear Zn(II)-containing center; however, recent studies have shown that human GLX2 contains a FeZn center, similar to that reported for *Arabidopsis* GLX2-5 (17).

GLX2-1 is unique among GLX2-like enzymes in that it has an Arg instead of a metal binding His at position 246 (Figure 2)(1,15). Although GLX2-1 and GLX2-5 share ~80% amino acid sequence identity and ~88% amino acid sequence similarity, we recently showed that recombinant GLX2-1 does not hydrolyze SLG or a number of other GLX2 substrates (18). Therefore, GLX2-1 is not a GLX2 isozyme. Our studies did however show that GLX2-1 exhibits β-lactamase activity and still binds two equivalents of metal.

The crystal structure of human GLX2 complexed with a slowly-processed substrate revealed that eight active site amino acids make considerable contacts with the substrate. Five of these amino acids (Lys217, Tyr219, Tyr248, Arg325, and Lys328) (19,20), which are conserved in GLX2-5 and in other GLX2's, are absent in GLX2-1. We were therefore interested in determining which of these amino acids are most important for GLX2 activity and predicted that we could introduce GLX2 activity into GLX2-1 by generating site-directed mutants of GLX2-1 containing the substrate/metal binding amino acids that are present in human GLX2. Enzymes containing single and multiple amino acid substitutions were generated and the resulting mutants were over-expressed, purified, and characterized using metal analyses, fluorescence spectroscopy, and steady-state kinetics to evaluate how these residues affect metal binding, structure, and catalysis. Our data show that two amino acid substitutions R246H and N248Y were enough to generate S-lactoylglutathione hydrolase activity.

Experimental Procedures

Homology Modeling

Molecular modeling of GLX2-1 was carried out using the SWISS-MODEL program (http://swissmodel.expasy.org) in conjunction with the Swiss PdbViewer, DeepView (http://www.expasy.org/spdbv/). A homology model of GLX2-1 was constructed using the NCBI sequences (http://www.ncbi.nlm.nih.gov) and modeling against the pdb structures 1XM8 (*Arabidopsis thaliana* GLX2 gene AT2G31350), 1QH5 (human GLX2 with S-(N-hydroxy-N-bromophenylcarbamoyl)glutathione), and 2Q42 (ensemble refinement of the protein crystal structure of *Arabidopsis thaliana* GLX2 gene At2g31350). Model generation was performed in Project mode using the sequence alignment seen in Figure 2. The project

file was submitted to the server, and the resulting structure was evaluated using ProSA-web (Z-score 1.04). The metal centers coordinates were duplicated from 1XM8 and measured for ligand-metal distance consistency between the model and template structures. The resulting structure was utilized without further refinement. Distance measurements and rotamer confirmations were calculated and images were generated using UCSF Chimera (http://www.cgl.ucsf.edu/chimera).

Generation of GLX2-1 active site mutations and the H238R mutant of GLX2-5

The N-terminus of over-expressed GLX2-1 was chosen to be identical to that for *A. thaliana* GLX2-5(1,18). The QuikChange site-directed mutagenesis kit was used to make the R246H , R 246H/N248Y, R246H/N248Y/Q325R/R328K, and R246H/N248Y/Q325R/R328K/S219F mutants of GLX2-1 and the H238R mutant of GLX2-5. PCR was conducted on either *GLX2-1/pT7-7* or *GLX2-5/pT7-7* with the primers shown in Table 1 to generate the mutants. DNA sequencing using the T7 promoter and T7 terminator primers was used to confirm the resulting mutations. The resulting plasmids were transformed into *E. coli* BL21(DE3) cells for over-expression studies. The co-expression plasmid, pGroESL, was transformed into BL21(DE3) *E. coli* cells containing *H238RGLX2-5/pT7-7* to assist in proper protein folding.

Over-expression and purification of GLX2-1 and GLX2-5 mutant enzymes

A 10 mL overnight culture of BL21(DE3) *E. coli* containing the R246H, R246H/N248Y, R246H/N248Y/G325R/G328K, and R246H/N248Y/G325R/G328K/S219F forms of *pGLX2-1/pT7-7* was used to inoculate 1L of LB (Luria Bertani) medium containing ampicillin (150 μg/mL), 250 μM $Fe(NH_4)_2(SO_4)_2$, and 250 μM $Zn(SO_4)_2$. The cells were grown, induced for protein over-expression, and harvested as previously described (18). For over-expression of the GLX2-5 H238R mutant, the pGroESL plasmid was transformed into the *E. coli* BL21(DE3) cells containing the *H238RGLX2-5/pT7-7* plasmid and over-expressed as described above.

Purification of all mutants was accomplished using previously published procedures (18). Protein purity was ascertained by using sodium dodecyl sulfate-polyacrylamide gel electrophoresis (SDS-PAGE). Enzyme containing fractions (8 mL) were pooled and concentrated by using an Amicon ultrafiltration cell equipped with a YM-10 membrane. Enzyme concentrations were determined by measuring the absorbance at 280 nm and using a molar extinction coefficient of 25,400 $M^{-1}cm^{-1}$(18).

Metal Analyses

The metal content of the enzymes was determined using an ICAP 61E Trace Analyzer (TJA: Thermo Jarrell Ash Corporation) with atomic emission spectroscopy detection (ICP-AES) as described previously (21). Protein samples were diluted to 10 μM with 10 mM MOPS, pH 7.2.

To evaluate metal binding to wild-type GLX2-1 and the mutant forms of the enzyme, a 3-fold molar excess of $Zn(SO_4)_2$ or $Fe(NH_4)_2(SO_4)_2$ or 1.5-fold molar excess of both $Fe(NH_4)_2(SO_4)_2$ and $Zn(SO_4)_2$ was added directly to the as-isolated enzymes, and the mixtures were allowed to incubate on ice for 1 hour. Unbound or loosely-bound metal ions were removed by 6 × 1L dialysis steps against 10 mM MOPS, pH 7.2, at 4 °C (12 h for each step). The metal content of these samples was determined using ICP-AES as described above.

Preparation of Co(II)-substituted GLX2-1 R246H

The metal-free (apo) R246H version of GLX2-1 was prepared by dialyzing a 0.1 mM solution of the protein against 4×2L of 10 mM 1,10 phenanthroline in 10 mM MOPS, pH 6.5, at 4 °C, followed by dialysis versus 6×1L of Chelex-treated, 10 mM MOPS, pH 6.5, at 4 °C. ICP-AES was used to confirm that the sample was metal-free. $CoCl_2$ was added directly to the sample to generate the Co(II)-substituted protein.

NMR Studies

^{1}H NMR spectra were collected on a Bruker Avance 500 spectrometer operating at 500.13 MHz, 298 K, magnetic field of 11.7 T, recycle delay (AQ) of 41 ms, and sweep width of 400 ppm. Chemical shifts were referenced by assigning the H_2O signal the value of 4.70 ppm. A modified presaturation pulse sequence (zgpr) was used to suppress the proton signals originating from solvent and amino acids not coupled to the metal center. The concentration of protein was ~ 1 mM, and 10% D_2O was included in samples for locking.

Steady state kinetics

The steady state kinetic parameters (K_m, k_{cat}) of the wild-type GLX2-1, GLX2-5 and the GLX2 variants were determined using S-*D*-lactoylglutathione (SLG) as the substrate. SLG hydrolysis was monitored at 240 nm over 30 s at 25 °C as previously reported (21). The concentration of GLX2 in the samples was typically 1-10 nM, and substrate concentrations ranged between 30 and 600 μM. The buffer used in the steady-state kinetic studies was 10 mM MOPS, pH 7.2.

Fluorescence spectra of the GLX2-1 variants

A Perkin-Elmer LS55 Luminescence spectrometer, tuned to an excitation wavelength of 295 nm and emission wavelength of 340 nm with a slit width of 5 nm, was used to monitor fluorescence emission intensities of the mutants. A 4 mm quartz cuvette was used, and the protein concentrations were 10 μM. Chelex-treated 10 mM MOPS, pH 7.2, was used as a buffer blank.

EPR Studies of GLX2-5 H238R

EPR spectra were recorded using a Bruker E600 EleXsys spectrometer equipped with an Oxford Instruments ESR900 helium flow cryostat and ITC503 temperature controller, and an ER4116DM cavity operating at 9.63 GHz in perpendicular mode. Other recording parameters are given in the legend to Figure 6. Quantitation of signals was carried out by double integration of spectra recorded at non-saturating power (2 mW) at 12 K. A 2 mM Cu(II)-EDTA standard in HEPES, pH 7.5, recorded at 60 K, 50 μW was used. Integration limits and correction factors for $S = 1/2$, and $S = 5/2$ signals where D is assumed to be small compared to temperature, were used as employed elsewhere (22) and recently described explicitly by Bou-Abdallah and Chasteen and references therein (23,24)). Computer simulations of EPR spectra were carried out using XSophe (25).

Results

Homology Modeling

We previously showed that GLX2-1 contains a dinuclear metal center even though the enzyme contains an Arg in place of a His in the conserved β-lactamase metal binding ligands (18). This raised the question of whether the GLX2-1 structure is significantly different from a typical GLX2 enzyme or if subtle structural alterations might position a more typical metal-binding ligand near the metal center. We have attempted to crystallize the enzyme and perform a structural analysis to answer this question. Unfortunately these

studies have been unsuccessful to date; therefore, modeling studies were undertaken to investigate these questions. Modeling of GLX2-1 against human GLX2 and *A. thaliana* GLX2-5 rendered a virtually identical tertiary structure for GLX2-1 as compared to the other two enzymes (Figure 3). This is not surprising given the high sequence conservation between the enzymes (human: 35% identity, 53% similarity and GLX2-5: 74% identity, 85% similarity). However, the model unexpectedly predicted that Arg246, which is a metal binding His in GLX2-2, GLX2-5, and human GLX2, is positioned directly over the Zn_2 metal binding site and is within binding distance of the metal ion in that site. The modeling prediction that Arg246 could bind a metal ion in the Zn_2 site is in contrast to our recent results that show that the R246L mutant of GLX2-1 binds 2 equivalents of metal. Nonetheless, the predicted position of Arg246 in the GLX2-1 model suggests that this residue restricts access of the substrate to the Zn_2 metal binding site. The model does not show any other potential metal binding ligands in the vicinity of the Zn(II), suggesting that the positive charge on Arg246 must be neutralized if it coordinates a metal ion.

The computer model of GLX2-1 also predicted that many of the key residues utilized for substrate binding in human GLX2 are different in GLX2-1 (Figure 3). Most notably, GLX2-1 has an asparagine at position 248, whereas human GLX2 contains a tyrosine that hydrogen bonds to the thioether of the substrate (15). In addition, human GLX2 contains an Arg at position 326 that hydrogen bonds to the carboxyl terminus of the substrate, while the model of GLX2-1 shows the presence of a glutamine at the same position. The GLX2-1 model did not reveal other residues in close proximity to the putative substrate-binding site that could accommodate the loss of these substrate-binding residues. Therefore, we hypothesized that the lack of catalytic activity exhibited by GLX2-1 (18) is due to the inability of the protein to bind SLG. To test this hypothesis, site-directed mutants of GLX2-1 were generated and characterized.

Over-expression and purification of GLX2-1 variants

The R246H, N248Y, R246H/N248Y, R246H/N248Y/Q325R/R328K, and R246H/N248Y/Q325R/R328K/S219F mutants were generated using site-directed mutagenesis, and the resulting mutations were confirmed by DNA sequencing. Since Gln325 and Arg328 are so close in the protein sequence, we used a single primer to generate the R246H/N248Y/Q325R/R328K mutant, rather than preparing triple mutants. The mutant enzymes were over-expressed and purified as soluble proteins. Approximately 25-30 mg of colorless protein was obtained from one liter of culture for wild-type GLX2-1 and each of the GLX2-1 mutant enzymes.

Metal Analyses

To determine if the mutations affected metal binding, the metal content of the purified GLX2-1 mutant enzymes was measured using ICP-AES. When wild-type GLX2-1 is over-expressed in LB medium containing 250 μM $Fe(NH_4)_2(SO_4)_2$ and 250 μM $Zn(SO_4)_2$, enzyme containing equal, albeit less than stoichiometric, amounts of Fe and Zn(II) was obtained (18) (Table 2). In contrast the GLX2-1 R246H enzyme contained nearly 2 equivalents of Zn(II) and undetectable amounts of Fe. The purified N248Y mutant contained very little metal and its fluorescence spectrum suggested significant amounts of unfolded protein (data not shown). All of the other mutants that contained the R246H mutation were isolated containing various amounts of Zn(II) and little or no Fe (Table 2).

We further investigated the ability of the GLX2-1 variants to bind metal by the addition of metal to the purified proteins followed by extensive dialysis to remove loosely-bound or unbound metal. The addition of a 3-fold molar excess of $ZnSO_4$ or $Fe(NH_4)_2(SO_4)_2$ to wild-type GLX2-1 resulted in analogs that bind nearly 2 equivalents of the metal that was added.

The addition of a 1.5-fold molar excess of both $Fe(NH_4)_2(SO_4)_2$ and $ZnSO_4$ to wild-type GLX2-1 resulted in an analog that binds equal amounts of Fe and Zn(II), with a total metal content greater than 3 equivalents, suggesting some nonspecific binding of metal.

The addition of a 3-fold molar excess of $ZnSO_4$ to the GLX2-1 mutant enzymes resulted in analogs that bound only Zn(II) at levels ranging from 1.4 to 2.4 equivalents (Table 2). The addition of a 3-fold molar excess of $Fe(NH_4)_2(SO_4)_2$ to the GLX2-1 mutant enzymes resulted in analogs that bound up to 4 equivalents of Fe yet retained significant amounts of Zn(II) binding. This result suggests that His246 in the GLX2-1 metal binding site confers a preference for Zn(II) to at least one site, even in the presence of excess Fe. In addition, this result suggests that the R246H mutation generates additional Fe binding sites since all of the GLX2-1 mutant enzymes containing the R246H mutation can bind up to four equivalents of total metal.

NMR spectroscopy on GLX2-1 R246H

To identify the metal binding ligands in the R246H GLX2-1 enzyme, ^{1}H NMR spectra were obtained on the Co(II)-substituted protein (2Co-R246H GLX2-1). The ^{1}H NMR spectrum of 2Co-R246H GLX2-1 in 10% D_2O revealed six paramagnetically-shifted resonances in between 20 and 80 ppm (Figure 4). The peak at 63 ppm integrated to 2 protons, while the peaks at 49, 44, 28, and 21 ppm integrated to 1 proton each, and the peak at 31 ppm integrated to slightly less than 1 proton. The spectrum of the same enzyme in 90% D_2O showed that the peaks at 63, 49, and 44 disappear and that the peak at 28 ppm is reduced in intensity by one-half. These solvent-exchangeable resonances can be readily assigned to N-H protons on Co(II)-bound histidines. This result indicates that there are 5 histidines bound to Co(II) in 2Co-R246H GLX2-1 and strongly suggests that the introduced His at position 253 binds metal.

Steady-state kinetics

Steady-state kinetic studies using SLG as the substrate were performed on the as-isolated GLX2-1 mutant enzymes to determine if any of the mutations resulted in an active enzyme. The R246H mutant, which was generated to yield a GLX2-1 variant with the same metal binding ligands as human GLX2 and GLX2-5, did not hydrolyze SLG (Table 2). On the other hand, the R246H/N248Y enzyme was active towards SLG and exhibited a k_{cat} of 2.1 ± 0.2 s^{-1} and a K_m of 295 ± 40 μM. The k_{cat} value for this enzyme is 86-fold lower than that of wild-type GLX2-5 (Table 2). Introduction of the Q325R/R328K mutations into the R246H/N248Y enzyme to yield the R246H/N248Y/Q325R/R328K mutant resulted in an enzyme that exhibited a k_{cat} value of 17 ± 2 s^{-1} and a K_m value of 249 ± 31 μM. The k_{cat} value of this enzyme is roughly 10-fold lower than that of GLX2-5 (Table 2). The introduction of a fifth mutation (S219F) to the R246H/N248Y/Q325R/R328K enzyme did not appreciably change the kinetic properties of the enzyme (Table 2).

To further evaluate the catalytic activity of the GLX2-1 variants, the metal-loaded enzymes were used in steady-state kinetic studies. The R246H form of GLX2-1 was not active independent of whether it had been incubated with Zn(II), Fe, or Zn/Fe (Table 2). In contrast, the R246H/N248Y variant of GLX2-1 exhibited a 10-fold increase in k_{cat}, as compared to that of the as-isolated enzyme, when the enzyme contained ≥ 2 equivalents of total metal. The metal-loaded R246H/N248Y/Q325R/R328K variant of GLX2-1 exhibited slightly higher k_{cat} values than that of the as-isolated enzyme, and metal-loaded R246H/N248Y/Q325R/R328K/S219F GLX2-1 exhibited an even smaller change in k_{cat} as compared to that of the as-isolated enzyme. The K_m values exhibited by the enzymes were not largely affected the amount or the identity of the metal ions bound to the catalytically-active analogs (Table 2).

Fluorescence spectra of GLX2-1 variants

Fluorescence spectra were obtained to ascertain whether the point mutations caused changes in the tertiary structure of the various forms of GLX2-1 (20) (Figure 5). The GLX2-1 R246H enzyme exhibited a fluorescence emission spectrum similar to that of the wild-type enzyme, suggesting that the substitution did not result in a large change in the environment around the tryptophans of the enzyme. The fluorescence emission spectrum of the R246H/N248Y variant was slightly higher than that of wild-type GLX2-1, which is expected if the additional Tyr at position 248 contributes to the overall fluorescence of the enzyme. In contrast, the R246H/N248Y/Q325R/R328K and R246H/N248Y/Q325R/R328K/S219F variants exhibited significantly increased fluorescence emission intensities, as compared to wild-type GLX2-1. This result suggests that the intrinsic fluorescence of one or more of the tryptophans in wild-type GLX2-1 is quenched, and the substitutions cause a change in structure that alleviates this quenching. The fact that the enzymes are catalytically-active and bind metal ions argues against the substitutions causing an unfolding of the protein.

Over-expression, purification, and characterization of Arabidopsis GLX2-5 H238R

Marasinghe *et al.* showed that mitochondrial *Arabidopsis* GLX2-5 exhibits glyoxalase 2 activity, and the recombinant enzyme was shown to bind 2 eq. of metals per enzyme (1). The crystal structure of GLX2-5 showed that His238 is a metal binding ligand (1). Our recent studies showed that GLX2-1, which contains an Arg at position 246 binds two metal ions (18). Therefore we reasoned that another as yet unidentified amino acid is recruited as a metal binding ligand in the Zn_2 binding site. However, the computational model of GLX2-1 predicted that the guanidinium amine of this arginine is positioned within 2.3 Å of the Zn_2 metal site, which is well within bonding distance (Figure 3). Furthermore, the R246H variant of GLX2-1 exhibited vastly differing metal binding properties as compared to wild-type GLX2-1, suggesting that Arg246 affects metal binding. Therefore to probe potential roles Arg could play in metal binding or catalysis, we mutated His238 in GLX2-5 to an Arg and evaluated the catalytic and metal binding properties of the resulting enzyme.

When the GLX2-5 H238R enzyme was over-expressed using standard over-expression conditions (1,18), the resulting enzyme was insoluble. Therefore, the co-expression plasmid, pGroESL, was introduced into the over expression cell line to assist in proper protein folding. When over expression of GLX2-5 H238R was performed in the presence of 250 μM $Fe(NH_4)_2(SO_4)_2$ and 250 μM $Zn(SO_4)_2$ using the pGroESL-containing system, we obtained approximately 20-25 mg of soluble, purple protein per liter of culture. This result suggests that His238 is important for the proper folding of GLX2-5, possibly by binding to the metal ion as the protein folds.

The GLX2-5 variant was found to bind 0.7 ± 0.2 equivalents of Fe and 0.6 ± 0.2 equivalents of Zn(II) and to exhibit a k_{cat} value of 0.32 ± 0.04 s^{-1} and a K_m value of 303 ± 79 μM when SLG was used as substrate (Table 2). The H238R mutation makes the enzyme approximately 600-fold less active than the wild-type GLX2-5 (Table 2). When as-isolated GLX2-5 H238R was incubated with a 1.5-fold molar excess of $Fe(NH_4)_2(SO_4)_2$ and $Zn(SO_4)_2$, and the mixture was exhaustively dialyzed versus Chelex-treated buffer, the resulting protein was shown to bind 1.1 ± 0.1 eq. of Fe and 1.7 ± 0.1 eq of Zn(II). The metal-loaded enzyme exhibited a 100-fold increase in k_{cat}, as compared to the as-isolated GLX2-5 H238R enzyme, and a nearly 2-fold drop in K_m (Table 2). Nonetheless, the metal-loaded GLX2-5 H238R variant was still 6-fold less active than wild-type GLX2-5.

The fluorescence spectra of the H238R variant of GLX2-5 showed a much higher emission intensity than the wild-type GLX2-5 enzyme, suggesting a significant change in the environment of Trp166 (the only Trp in GLX2-5) or multiple Tyr's as a result of the

substitution (Figure 7). This change in environment would have to occur over a large distance as Trp166 is over 20 Å away from His238. This change in tertiary structure may explain the lower k_{cat} values of the mutant.

We initially hypothesized that the presence of an arginine at position 238 of GLX2-5 would disrupt the binuclear metal-binding center in the enzyme. However, given that the H238R variant of GLX2-5 can still bind two equivalents of metal, we interrogated metal binding to this enzyme using EPR spectroscopy (Figure 6). Three types of signals were exhibited by the enzyme. The predominant signal from the as-isolated enzyme was a $g_{eff.} \sim 4.3$ signal at 1605 G, due to $M_S = \pm 3/2$ of $S = 5/2$ Fe(III) (Figure 6B). Associated low field features due to the ground state $M_S = \pm 1/2$ were observed on the low-field side of the $g_{eff.} \sim 4.3$ resonance, ending abruptly at $g_{eff.} \sim 10$ (680 G). The signal is typical for low symmetry Fe(III) and does not confirm whether the iron associated with it is bound in a specific site in the mutant. A second signal observed in the spectrum was an apparently axial signal, though a preliminary simulation (not shown) suggested rhombic $g_{eff.}$ values of $g_{eff.} \sim 1.945$, 1.845 and 1.775. This signal was identical to a signal from GLX2-1 (Figure 6A) and is indicative of a mixed-valence Fe(II)-Fe(III) center. The signal was reasonably well-simulated (Figure 6C) by explicitly assuming spin-coupled $S = 5/2$ and $S = 2$ iron ions, with the ions 3.5 Å apart and experiencing an exchange coupling of 18 cm^{-1} (detailed parameters are given in the caption to Figure 6). While these values do not provide a unique solution, they nevertheless support the assignment. A third signal was observed that is common in the spectrum of as-isolated GLX2-1 (Figure 6A) and the metal-loaded H238R variant of GLX2-5 (Figure 6D), but not in the as-isolated H238R variant. The signal was best observed by subtraction of the spectrum of the as-isolated H238R variant of GLX2-5 from that of the enzyme after incubation with Fe and Zn(II) (Figure 6F). A computer simulation (Figure 6E) suggested a single Fe(III) ion with $S = 5/2$ and a less-than-completely rhombic zero field splitting, with $E/D = 0.2$. The discrete value for E/D, and the resolution of the three $g_{edf.}$ resonances of the $M_S = 3/2$ doublet, suggests a small distribution in zero field splitting parameters (low 'strains' in E) and, in turn, Fe(III) with a well-defined coordination such as would be expected for binding in the active site of an enzyme.

Discussion

The metallo-β-lactamase fold consists of an αβ/βα sandwich motif, made up of a core unit of two β-sheets surrounded by solvent-exposed helices (26). Members of this superfamily contain a conserved HXHXD motif that has been shown to bind Zn(II), Fe, and Mn (14,27,28). There are several enzymes in the metallo-β-lactamase fold superfamily, including: metallo-β-lactamases, glyoxalase 2, lactonase, rubredoxin:oxygen oxidoreductase (ROO), arylsulfatase, phosphodiesterase, and tRNA maturase (29). Most members of the metallo-β-lactamase superfamily (metallo-β-lactamases, tRNA maturase, phosphodiesterase, arylsulfatase, and lactonase) appear to contain dinuclear Zn(II) centers. On the other hand, rubredoxin:oxygen oxidoreductase (ROO) appears to contain a dinuclear iron center (30). Human GLX2 was reported to contain a dinuclear Zn(II) center (15); however, NMR and EPR studies recently showed that recombinant human GLX2 contains a Fe(II)Zn(II) center but that the catalytic activity is due to Zn(II) in the Zn_1 site (17). Plant mitochondrial GLX2 (GLX2-5) has been reported to contain a FeZn center (1), and plant cytoplasmic GLX2 can exist with a number of possible metal centers, including dinuclear Fe, FeZn, and presumably dinuclear Zn(II) centers (14,27). GloB, the GLX2 from *Salmonella typhimurium*, also is isolated containing mixtures of metal centers(31).

Arabidopsis GLX2-1 is highly similar to GLX2-5 and is clearly a member of the metallo-*β*-lactamase fold superfamily (26). However, GLX2-1 is unique in that it contains an Arg at position 246, which is a metal binding His in all other GLX2 enzymes (29). Metal analyses,

kinetic, and spectroscopic results demonstrated that GLX2-1 contains a dinuclear metal center; however, it does not exhibit glyoxalase 2 activity (18). In addition to the histidine to arginine substitution at position 246, five of the eight amino acids present at the active site of human GLX2 (Lys217, Tyr219, Tyr248, Arg325, and Lys328) (Figure 2), which are involved with substrate binding and are conserved in GLX2-2, GLX2-4, and GLX2-5 (18-20), are not conserved in GLX2-1. We predicted that one or more of these changes are responsible for the inability of GLX2-1 to bind and hydrolyze SLG. In an effort to test this hypothesis, we generated mutants of GLX2-1 that contained a His at position 246 and that contain some or all of the predicted GLX2-5 substrate binding ligands (Figure 3).

The Zn(II)-loaded R246H mutant of GLX2-1 tightly bound 2 equivalents of Zn(II). We used Co(II), which is an excellent surrogate for Zn(II) (32), to demonstrate that the Co(II) ions bind to the Zn_1 and Zn_2 sites in GLX2-1, including to the introduced His. After the R246H variant of GLX2-1 was made and characterized, the substrate binding amino acids of human GLX2 were introduced into the enzyme. The resulting enzymes were found to bind 0.5-1.2 equivalents of Zn(II), regardless of whether excess Fe or Zn(II) was added to the enzymes (Table 2). Interestingly, the enzymes also bound ≥ 1.9 equivalents of Fe if excess Fe was added to the proteins, suggesting that the R246H mutation exposes or creates additional Fe binding sites in GLX2-1. Fluorescence spectroscopy was used to evaluate whether the point mutations changed the tertiary structure of the GLX2-1 mutants. In all cases, the mutants exhibited similar or higher fluorescence emission than wild-type GLX2-1. This result indicates that the point mutations did not cause major folding alterations in the mutants but that the environment around one or more of Trp's in the mutants has changed relative to wild-type GLX2-1.

While replacement of Arg246 with a His had no effect on the ability of GLX2-1 to hydrolyze SLG, the metal-loaded analog of GLX2-1 R246H/N248Y exhibited significant SLG hydrolase activity (k_{cat} of 22 ± 2 s^{-1}; Table 2). In human GLX2, when Tyr175, which corresponds to Asn248 in GLX2-1 and Tyr240 in GLX2-5, was replaced by a phenylalanine, the resulting enzyme exhibited a 1.5-fold decrease in k_{cat} and an 8-fold increase in K_m (33). In the crystal structure of human GLX2, the hydroxyl group of Tyr175 is within hydrogen bonding distance of the amide nitrogen of the glutathione glycine, and this interaction is thought to be a significant contribution to the binding of substrate (33). Our data demonstrate that this single point mutation transforms GLX2-1 into a catalytically-active glyoxalase 2 enzyme.

We attempted to prepare the single N248Y GLX2-1 variant to evaluate whether this mutation alone would afford glyoxalase 2 activity to GLX2-1; however after purification, the N248Y variant contained only minor amounts of metal and the metal content could not be increased to the levels of wild-type GLX2-1 by addition of excess metals followed by dialysis. The fluorescence emission spectrum of the enzyme suggested that it contained significant amounts of unfolded protein. We do not know the reason for this result; however, the computational model of GLX2-1 suggests that there could be steric problems with a tyrosine at position 248 when an arginine is at position 246 (Figure 3).

The role of several predicted SLG binding ligands was tested by introducing two additional mutations into GLX2-1 R246H/N248Y to generate the GLX2-1 R246H/N248Y/Q325R/R328K variant. The metal-loaded form of this enzyme exhibited a 1.7-fold increase in k_{cat} and a 1.3-fold decrease in K_m, as compared to GLX2-1 R246H/N248Y (Table 2). This result is consistent with the fact that the rate-limiting step for GLX2 is substrate binding (34). Phe145, which corresponds to Ser219 in GLX2-1, was previously predicted to be involved in the binding of substrate to human GLX2; however, the introduction of a phenylalanine

(S219F) to the GLX2-1 R246H/N248Y/Q325R/R328K enzyme did not further increase k_{cat} or decrease K_m, suggesting that this residue does not play a major role in substrate binding.

In order to further test if metal binding to His238 is involved in catalysis, we prepared the H238R mutant of GLX2-5. Like GLX2-1, the as-isolated H238R version of GLX2-5 binds significant amounts of metal, and a metal-loaded form with > 2 eq. of total metal could be generated (Table 2). EPR spectra suggest that the mutant contains a metal site similar to that of the wild-type enzyme. However, this metal-loaded analog exhibited a k_{cat} that is nearly 6-fold less than wild-type GLX2-5. This result suggests that in addition to its role as a metal binding ligand, His238 may play a role in catalysis, possibly by orienting Tyr240 for proper substrate binding (Figure 3). However, some of the lost activity may be due to changes in the geometry/orientation of the metal center and/or the possibility that the H238R mutant is not as stable as the wild-type enzyme. The fluorescence spectrum of the GLX2-5 H238R enzyme showed a shoulder at 390 nm, suggesting that some of the protein in this sample was partially-unfolded (Figure 7). In addition, the GLX2-5 H238R enzyme, unlike wild-type GLX2-5, was not stable to solvent exchange in NMR experiments (data not shown). These results suggest that along with metal binding, His253 may have a role in catalysis and stability in GLX2 enzymes.

One of the common, albeit surprising, aspects of the GLX2's is that many of the analogs bind more than two metal ions (see Table 2 as an example) (14,27,35). In an effort to identify any potential metal binding sites on GLX2-1, the homology model (Figure 3) was probed for any potential metal binding sites. A possible site, consisting of His179, Asp96, and Asp98, was identified (Figure 8 (left)). These same residues are conserved in GLX2-5 but not in human GLX2 (Figure 2). Interestingly, a remote metal binding site was also reported in human GLX2, consisting of His185, His235, and Glu251 (Figure 8 (right))(15). It is not clear if these remote metal binding sites affect structure/function of the GLX2's.

Abbreviations

EDTA	ethylenediaminetetraacetic acid
ICP-AES	inductively-coupled plasma with atomic emission spectroscopy
LB	Luria-Bertani
MOPS	3-(N-morpholino)propanesulfonic acid
SLG	S-*D*-lactoylglutathione

References

1. Marasinghe GPK, Sander IM, Bennett B, Periyannan G, Yang KW, Makaroff CA, Crowder MW. Structural studies on a mitochondrial glyoxalase II. J. Biol. Chem. 2005; 280:40668–40675. [PubMed: 16227621]
2. Thorson JS, Chapman E, Schultz PG. Analysis of Hydrogen Bonding Strengths in Proteins Using Unnatural Amino Acids. J. Am . Chem . Soc. 1995; 117:9361–9362.
3. Thornalley PJ. Pharmacology of Methylglyoxal: Formation, Modification of Proteins and Nucleic Acids, and Enzymatic Detoxification--A Role in Pathogenesis and Antiproliferative Chemotherapy. Gen. Pharmacol. 1996; 27:565–573. [PubMed: 8853285]
4. Thornalley PJ. Methylglyoxal, Glyoxalases and the Development of Diabetic Complications. Amino Acids. 1994; 6:15–23.
5. Thornalley PJ. Modification of the Glyoxalase System in Disease Processes and Prospects for Therapeutic Strategies. Biochem. Soc. Trans. 1993; 21:531–534. [PubMed: 8359526]

6. Vander Jagt DL. Glyoxalase II: Molecular Characteristics, Kinetics, and Mechanism. Biochem. Soc. Trans. 1993; 21:522–527. [PubMed: 8359524]
7. Uotila L. Purification and Characterization of S-2-Hydroxyacylglutathione Hydrolase (Glyoxalase II) from Human Liver. Biochemistry. 1973; 12:3944–3951. [PubMed: 4745654]
8. Creighton DJ, Hamilton DS. Brief History of Glyoxalase I and What We Have Learned about Metal Ion Dependent, Enzyme Catalyzed Isomerizations. Arch. Biochem. Biophys. 2001; 387:1–10. [PubMed: 11368170]
9. Cordell PA, Futers TS, Grant PJ, Pease RJ. The Human Hydroxyacylglutathione Hydrolase (HAGH) Gene Encodes Both Cytosolic and Mitochondrial Forms of Glyoxalase II. J. Biol. Chem. 2004; 279:28653–28661. [PubMed: 15117945]
10. Maiti MK, Krishnasamy S, Owen HA, Makaroff CA. Molecular Cloning of Glyoxalase II from a Higher Plant: Comparison of Mitochondrial and Cytoplasmic Isozymes. Plant Mol. Biol. 1997; 35:471–481. [PubMed: 9349270]
11. Thornalley P. The Glyoxalase System in Health and Disease. Mol. Aspects Medicine. 1993; 14:287–371.
12. Thornalley P. Advances in Glyoxalase Research. Glyoxalase Expression in Malignancy, Anti-Proliferative Effects of Methylglyoxal, Glyoxalase I Inhibitor Diesters, and S-*D*-Lactoylglutathione, and Methylglyoxal-Modified Protein Binding and Endocytosis by the Advanced Glycation Endproduct Receptor. Crit. Rev. Oncol. Hematol. 1995; 20:99–128. [PubMed: 7576201]
13. Schilling O, Vogel A, Meyer-Klaucke W. EXAFS studies on proteins from the metallo-β-lactamase family reveal similar metal sites in an oxido-reductase and the hydrolase ElaC. J. Inorg. Biochem. 2001; 86:422.
14. Wenzel NF, Carenbauer AL, Pfiester MP, Schilling O, Meyer-Klaucke W, Makaroff CA, Crowder MW. The binding of iron and zinc to glyoxalase II occurs exclusively as di-metal centers and is unique within the metallo-β-lactamase family. J. Biol. Inorg. Chem. 2004; 9:429–438. [PubMed: 15067523]
15. Cameron AD, Ridderstrom M, Olin B, Mannervik B. Crystal Structure of Human Glyoxalase II and its Complex with a Glutathione Thiolester Substrate Analogue. Structure. 1999; 7:1067–1078. [PubMed: 10508780]
16. Ullah AHJ, Dischinger HC. Identification of Active Site Residues in *Aspergillus ficuum* Extracellular pH 2.5 Optimum Acid Phosphatase. Biochem. Biophys. Res. Commun. 1993; 192:754–759. [PubMed: 8484781]
17. Limphong P, McKinney RM, Adams NE, Bennett B, Makaroff CA, Gunasekera TS, Crowder MW. Human glyoxalase II contains an Fe(II)Zn(II) center but is active as a mononuclear Zn(II) enzyme. Biochemistry. 2009; 48:5426–5434. [PubMed: 19413286]
18. Limphong P, Crowder MW, Bennett B, Makaroff CA. *Arabidopsis thaliana* GLX2-1 contains a dinuclear site but is not a glyoxalase 2. Biochem. J. 2009; 417:323–330. [PubMed: 18782082]
19. Cameron AD, Olin B, Ridderstrom M, Mannervik B, Jones TA. Crystal Structure of Human Glyoxalase I -- Evidence for Gene Duplication and 3D Domain Swapping. EMBO J. 1997; 16:3386–3395. [PubMed: 9218781]
20. Zang TM, Hollman DA, Crawford PA, Crowder MW, Makaroff CA. Arabidopsis Glyoxalase II Contains a Zinc/Iron Binuclear Metal Center That Is Essential for Substrate Binding and Catalysis. J. Biol. Chem. 2001; 276:4788–4795. [PubMed: 11085979]
21. Crowder MW, Maiti MK, Banovic L, Makaroff CA. Glyoxalase II from *A. thaliana* Requires Zn(II) for Catalytic Activity. FEBS Lett. 1997; 418:351–354. [PubMed: 9428743]
22. Purpero VM, Moran GR. Catalytic, noncatalytic, and inhibitory phenomena: kinetic analysis of (4-hydroxyphenyl)pyruvate dioxygenase from *Arabidopsis thaliana*. Biochemistry. 2006; 45:6044–6055. [PubMed: 16681377]
23. Bou-Abdallah F, Chasteen ND. Spin concentration measurements of high-spin (g ’=4.3) rhombic iron(III) ions in biological samples: theory and application. J. Biol. Inorg. Chem. 2008; 13:15–24. [PubMed: 17932693]
24. Aasa R, Vanngard T. EPR Signal Intensity and Powder Shapes: A Reexamination. J. Mag. Res. 1975; 19:308–315.

25. Hanson, GR.; Gates, KE.; Noble, CJ.; Mitchell, A.; Benson, S.; Griffin, M.; Burrage, K. EPR of Free Radicals in Solids: Trends in Methods and Applications. Shiotani, M.; Lund, A., editors. Kluwer Press; New York: 2003. p. 197-237.
26. Melino S,C,C, Dragani B, Aceto A, Petruzzelli R. A Zinc Binding Motif Conserved in Glyoxalase II, β-lactamases, and Arylsulfatases. Trends Biochem. Sci. 1998; 23:381–382. [PubMed: 9810225]
27. Schilling O, Wenzel N, Naylor M, Vogel A, Crowder M, Makaroff C, Meyer-Klaucke W. Flexible metal binding of the metallo-β-lactamase domain: Glyoxalase II incorporates iron, manganese, and zinc *in vivo*. Biochemistry. 2003; 42:11777–11786. [PubMed: 14529289]
28. Campos-Bermudez VA, Moran-Barrio J, Costa-Filho AJ, Vila AJ. Metal-independent inhibition of glyoxalase II: A possible mechanism to regulate the enzyme activity. J. Inorg. Biochem. 2010; 104:726–731. [PubMed: 20385411]
29. Bebrone C. Metallo-β-lactamases (classification, activity, genetic organization, structure, zinc coordination) and their superfamily. Biochem. Pharmacol. 2007; 74:1686–1701. [PubMed: 17597585]
30. Frazao C, Silva G, Gomes CM, Matias P, Coelho R, Sieker L, Macedo S, Liu MY, Oliveira S, Teixeira M, Xavier AV, Rodrigues-Pousada C, Carrondo MA, Le Gall J. Structure of a dioxygen reduction enzyme from *Desulfovibrio gigas*. Nature Structural Biol. 2000; 7:1041–1045.
31. Campos-Bermudez VA, Leite NR, Krog R, Costa-Filho AJ, Soncini FC, Oliva G, Vila AJ. Biochemical and structural characterization of *Salmonella typhimurium* glyoxalase II: New Insights into metal ion selectivity. Biochemistry. 2007; 46:11069–11079. [PubMed: 17764159]
32. Maret, W.; Vallee, BL. Meth. Enzymol. Academic Press; New York: 1993. p. 52-71.
33. Ridderstrom M, Jemth P, Cameron AD, Mannervik B. The Active Site Tyr-175 in Human Glyoxalase II Contributes to Binding of Glutathione Derivatives. Biochim. Biophys. Acta. 2000; 1481:344–348. [PubMed: 11018726]
34. Creighton DJ, Migliorini M, Pourmotabbed T, Guha MK. Optimization of Efficiency in the Glyoxalase Pathway. Biochemistry. 1988; 27:7376–7384. [PubMed: 3207683]
35. Limphong P, Crowder MW, Bennett B, Makaroff CA. *Arabidopsis thaliana* GLX2-1 contains a dinuclear metal binding site, but is not a glyoxalase 2. Biochem. J. 2009; 417:323–330. [PubMed: 18782082]

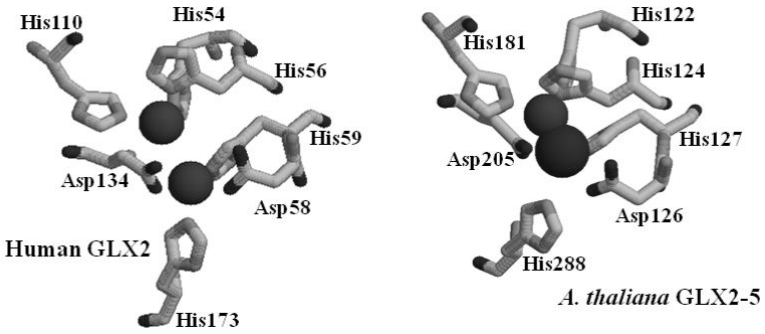

Figure 1.
Crystal structure of *Arabidopsis thaliana* GLX2-5 and human GLX2 (1,15). Numbering scheme corresponds to the sequences in Figure 2.

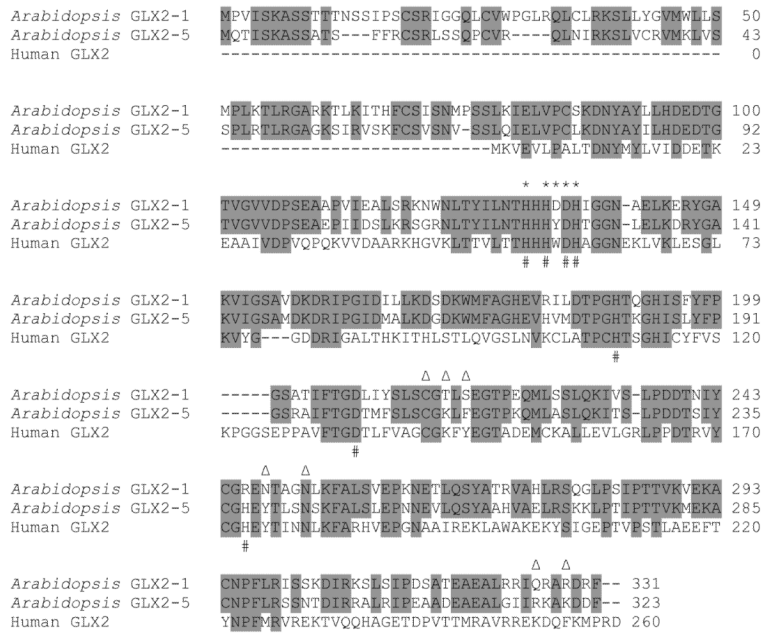

Figure 2.

Alignment of predicted plant glyoxalase II's from *A. thaliana*. The * marks the metallo-β-lactamase fold motif. The # marks the highly-conserved metal binding residues. The Δ marks the substrate binding residues.

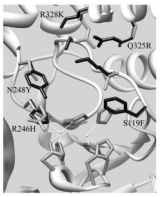

Figure 3.
Computational model of the active site of GLX2-1 overlapped with the active site of GLX2-5. Metal binding ligands are the same in both models except residue Arg246. Gray residues indicate the metal binding sites of GLX2-1, and black residues indicate the metal binding site of GLX2-5.

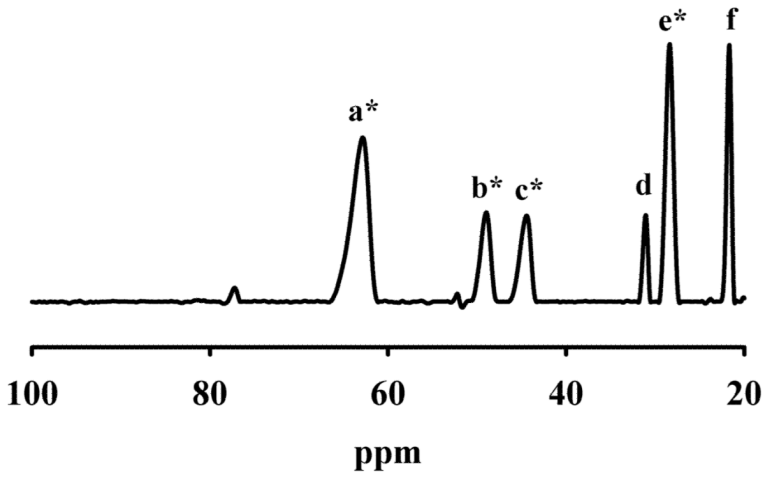

Figure 4.

^{1}H NMR spectrum of the 2Co-R246H mutant of GLX2-1 in 10 mM MOPS, pH 7.2, containing 10% D_2O. The enzyme concentration in the samples was ~ 1 mM. The * represents peaks that were solvent-exchangeable. Peak e in the spectrum decreased by 1/2 when the sample was exchanged in 90% D_2O.

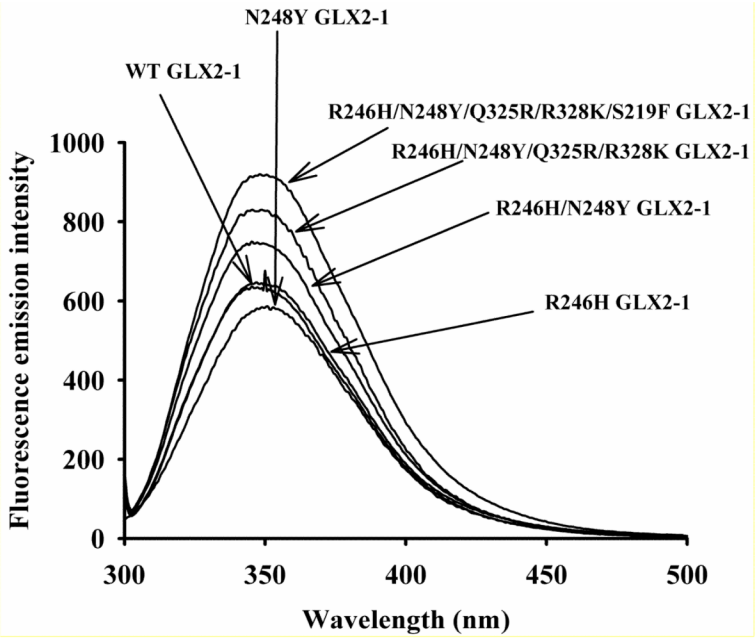

Figure 5.
Fluorescence emission spectra of wild-type GLX2-1 and GLX2-1 mutants. The concentration of samples was 10 μM, and the buffer was 10 mM MOPS, pH 7.2. An excitation wavelength of 295 nm was used.

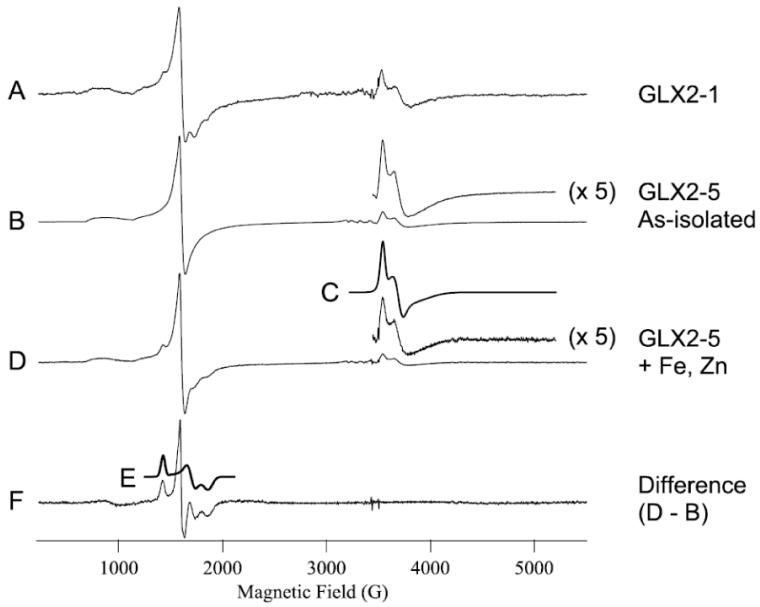

Figure 6.

EPR spectra from GLX2-1 and the H238R mutant of GLX2-5. (A) As-isolated wild-type GLX2-1. (B) As-isolated H238R mutant of GLX2-5. (C) Simulation of the $g_{\text{eff.}}$ = 1.775 - 1.945 signal, assuming interacting Fe(III) (S = 5/2, isotropic g = 2.0, D = 2 cm^{-1}, E/D = 1/3) and Fe(II) (S = 2, g = 1.92, 2.01 and 2.01, D = 15 cm^{-1}, E/D = 0.085), with $J_{\text{Fe(II)-Fe(III)}}$ = 18 cm^{-1} and an inter-iron distance $r_{\text{Fe(II)-Fe(III)}}$ = 3.5 Å. The discrepancy in lineshape at the high-field side of the middle resonance is likely due to broadening in the experimental spectrum due to strains in **D** and/or **J**. (D) H238R mutant of GLX2-5 after addition of 1.5 eq. Fe(II) and 1.5 eq. Zn(II). (E) Computed spectrum, assuming S = 5/2 (Fe(III)), g = 2, D = 1 cm^{-1}, E/D = 0.2. (F) Difference spectrum generated by subtraction of B from D. Experimental spectra were recorded at 2 mW microwave power, 10 K, and 12 G (1.2 mT) magnetic field modulation at 100 kHz.

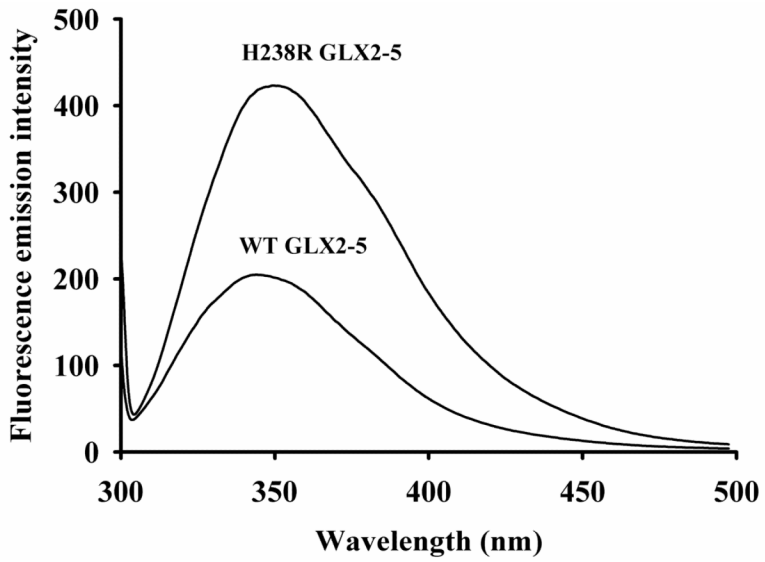

Figure 7.

Fluorescence emission spectra of wild-type GLX2-5 and the H238R mutant of GLX2-5. The concentration of samples was 10 μM, and the buffer was 10 mM MOPS, pH 7.2. An excitation wavelength of 295 nm was used.

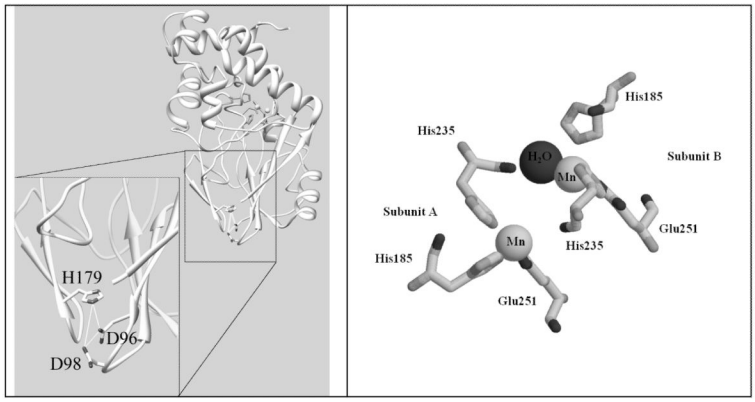

Figure 8.
(Left) Homology model of GLX2-1 showing a potential remote metal binding site consisting of Asp96, Asp98, and His179. (Right) Remote metal binding sites of human GLX2 on subunits A and B (15). The large dark sphere is a solvent molecule.

Table 1

Oligonucleotide primers for site-directed mutagenesis

Code	Comment	5′-3′ Nucleotide sequence
1021	R246H GLX2-1 forward	CAA ATA TAT ACT GCG GCC ATG AAA ACA CAG CAG GC
1022	R246H GLX2-1 reverse	GCC TGC TGT GTT TTC ATG GCC GCA GTA TAT ATT TG
1023	R246H/N248Y GLX2-1 forward	CAA ATA TAT ACT GCG GCC ATG AAT ACA CAG CAG GCA ATC TCA AG
1024	R246H/N248Y GLX2-1 reverse	CTT GAG ATT GCC TGC TGT GTA TTC ATG GCC GCA GTA TAT ATT TG
1025	R246H/N248Y/Q325R/R328K GLX2-1 forward	GAA GCA TTG CGT CGT ATA CGG AGA GCC AAA GAT CGT TTC
1026	R246H/N248Y/Q325R/R328K GLX2-1 reverse	GAA ACG ATC TTT GGC TCT CCG TAT ACG ACG CAA TGC TTC
1027	R246H/N248Y/Q325R/R328K/S219F GLX2-1 forward	CAA TAT TCA CAG GAG ACC TGA TAT TTA GCT TAT CCT GTG GTA C
1028	R246H/N248Y/Q325R/R328K/S219F GLX2-1 reverse	GTA CCA CAG GAT AAG CTA AAT ATC AGG TCT CCT GTG AAT ATT G
1029	H238R GLX2-5 forward	CAC AAG CAT ATA CTG TGG TCG TGA ATA TAC ACT GAG TAA TTC C
1030	H238R GLX2-5 reverse	GGA ATT ACT CAG TGT ATA TTC ACG ACC ACA GTA TAT GCT TGT G

Table 2

Metal content and steady-state kinetic constants for wild-type and mutant GLX2-1 and GLX2-5 analogs

Protein	k_{cat} (s^{-1})	K_m(μM)	k_{cat}/K_m ($\mu M^{-1}s^{-1}$)	Fe(eq)	Zn(eq)
wild-type GLX2-1					
As-isolated	N/A[a]	N/A	N/A	0.3±0.1[b]	0.3±0.2[b]
Zn(II) added[c]	N/A	N/A	N/A	~0.1[b]	1.6±0.2[b]
Fe(II) added[d]	N/A	N/A	N/A	1.9±0.1[b]	0.2±0.1[b]
Fe(II) and Zn(II) added[e]	N/A	N/A	N/A	1.6±0.2[b]	1.6±0.2[b]
R246H GLX2-1					
As-isolated	N/A	N/A	N/A	ND[c]	1.7±0.3
Zn(II) added[c]	N/A	N/A	N/A	ND	2.0±0.2
Fe(II) added[d]	N/A	N/A	N/A	3.3±0.3	1.2±0.2
Fe(II) and Zn(II) added[e]	N/A	N/A	N/A	0.8±0.3	1.7±0.3
R246H/N248Y GLX2-1					
As-isolated	2.1±0.2	295±40	0.007±0.005	0.2±0.1	1.2±0.2
Zn(II) added[c]	23±4	310±110	0.07 ±0.04	ND	2.4±0.1
Fe(II) added[d]	19±2	257±58	0.07 ±0.03	3.5±0.3	1.2±0.3
Fe(II) and Zn(II) added[e]	22±2	370±60	0.06 ±0.03	0.6±0.2	2.5±0.1
R246H/N248Y/Q325R/R328K GLX2-1					
As-isolated	17±2	249±31	0.07±0.05	ND	1.2±0.2
Zn(II) added[c]	30±2	238±41	0.12 ±0.05	ND	1.5±0.1
Fe(II) added[d]	22±2	290±59	0.07 ±0.04	1.9±0.2	1.2±0.3
Fe(II) and Zn(II) added[e]	38±5	285±78	0.13 ±0.06	1.1±0.1	1.5±0.1
R246H/N248Y/Q325R/R328K/S219F					
As-isolated	16±1	240±39	0.07±0.03	ND	1.1±0.3
Zn(II) added[c]	17±2	186±55	0.09 ±0.04	ND	1.4±0.1

Protein	k_{cat} (s^{-1})	K_m(μM)	k_{cat}/K_m ($\mu M^{-1}s^{-1}$)	Fe(eq)	Zn(eq)
Fe(II) added[d]	20±3	313±55	0.06±0.03	3.4±0.3	0.5±0.2
Fe(II) and Zn(II) added[e]	20±3	220±72	0.09 ±0.03	1.1±0.1	1.4±0.1
GLX2-5					
As-isolated wild-type	180±20	267±63	0.67±0.31	0.6±0.1	1.8±0.1
As-isolated H238R	0.32±0.04	303±79	0.001±0.001	0.7±0.2	0.6±0.2
Fe(II) and Zn(II) added[e]	31±2	194±32	0.16±0.7	1.1±0.1	1.7±0.1

[a] N/A – no activity

[b] previously published results (18)

[c] 3-fold excess of Zn(II) added after purification

[d] 3-fold excess of Fe(II) added after purification

[e] 1.5-fold excess of Fe plus 1.5-fold excess of Zn(II) added after purification

[f] ND – none detected

Biochemistry. Author manuscript; available in PMC 2011 September 21.